Large-eddy simulation of incompressible viscous fluid flows by the spectral element method

Roland Bouffanais†, Emmanuel Leriche† and Michel O. Deville†

†Laboratory of Computational Engineering (LIN)
École Polytechnique Fédérale de Lausanne
CH–1015 Lausanne
http://lin.epfl.ch

TI2006, May 2006

ÉCOLE POLYTECHNIQUE
FÉDÉRALE DE LAUSANNE

This research was partially funded by a Swiss National Science Foundation Grant (no. 200020–101707), whose support is gratefully acknowledged

Outline

Goal

To perform **large-eddy simulation (LES)** of

- 3D **turbulent Newtonian incompressible** fluid flows
- by **spectral element methods (SEM)**
  - geometrical flexibility of finite element methods
  - convergence and accuracy of spectral methods
- using various **subgrid-scale models**
  - dynamic Smagorinsky model (DSM)
  - dynamic mixed model (DMM)
  - approximate deconvolution model (ADM)
- relying on **fully-explicit filtering** techniques
  - relying on specific element-wise spectral filter

The lid-driven cavity flow at Re=12 000

Problem characteristics: 1/2

- 3D, unsteady, incompressible, viscous & Newtonian flows
- Uniform density and temperature
- No-slip boundary conditions on the bottom and side walls
- Lid-filtered velocity distribution:

$$u_0 = U_0 \left[1 - \left(\frac{x}{h}\right)^{18}\right]^2 \left[1 - \left(\frac{z}{h}\right)^{18}\right]^2$$

$$v_0 = w_0 = 0$$

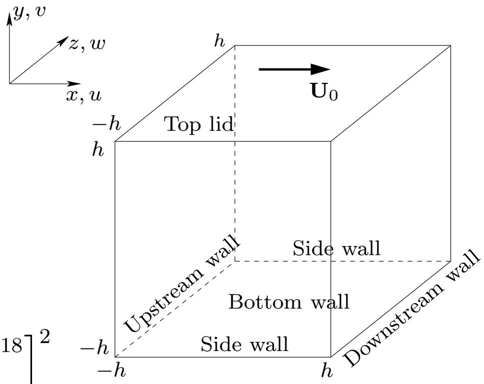

The lid-driven cavity flow at Re$=12\,000$

Problem characteristics: 2/2

- Flow governed by the filtered Navier–Stokes equations

$$\frac{\partial \overline{\mathbf{u}}}{\partial t} + \boldsymbol{\nabla} \cdot \overline{\mathbf{u}}\,\overline{\mathbf{u}} = -\boldsymbol{\nabla} \overline{p} + \nu \boldsymbol{\Delta} \overline{\mathbf{u}} - \boldsymbol{\nabla} \cdot \boldsymbol{\tau},$$
$$\boldsymbol{\nabla} \cdot \overline{\mathbf{u}} = 0,$$

  with $\overline{\mathbf{u}}$: filtered velocity field;
  $\overline{p} = \overline{P}/\rho$: filtered static pressure;
  ν: uniform kinematic viscosity

- The subgrid-scale (SGS) stress tensor $\boldsymbol{\tau} = \overline{\mathbf{u}\mathbf{u}} - \overline{\mathbf{u}}\,\overline{\mathbf{u}}$
  $\hookrightarrow$ accounting for the effects of the small-scales on the dynamics of the resolved-scales

Subgrid-scale modeling

Two fully-explicit filtering dynamic models

- Dynamic Smagorinsky model (DSM)
  - overcomes the difficulty of constant C_S in the Smagorinsky model
  - $C_\mathsf{d}(\mathbf{x},t)$ calculated based on the Germano–Lily dynamic procedure[1]

$$\boldsymbol{\tau}^\mathsf{d} = -2C_\mathsf{d}(\mathbf{x},t)\overline{\Delta}^2|\overline{\mathbf{S}}|\overline{\mathbf{S}} \quad \text{with} \quad |\overline{\mathbf{S}}| = (2\overline{S}_{ij}\overline{S}_{ij})^{1/2}$$

superscript "d" denotes the deviatoric part of the tensor

- Dynamic mixed model (DMM)
  - blend of the mixed model of Bardina and the DSM[2]
  - Bardina's mixed model is not an eddy-viscosity model: structural modal relying on the scale-similarity principle
  - produces almost no dissipation ⇒ needs to be used with DSM

$$\boldsymbol{\tau}^\mathsf{d} = \mathcal{L}^\mathsf{d} - 2C_\mathsf{d}(\mathbf{x},t)\overline{\Delta}^2|\overline{\mathbf{S}}|\overline{\mathbf{S}} \quad \text{with} \quad \mathcal{L} = \overline{\overline{\mathbf{u}}\,\overline{\mathbf{u}}} - \overline{\overline{\mathbf{u}}}\,\overline{\overline{\mathbf{u}}}$$

[1] Lilly, D. K., A proposed modification of the Germano subgrid-scale closure method. *Phys. Fluids A*, **4**, 633–635, 1992.

[2] Zang, Y., Street, R. L. & Koseff, J. R. A dynamic mixed subgrid-scale model and its application to turbulent recirculating flows. *Phys. Fluids A*, **5**, 3186–3193, 1993.

Spatial discretization – Time integrators

- Galerkin approx. of the weak filtered Navier–Stokes Eqs. based on the **Legendre spectral element method** (SEM) using a **staggered mesh** $\mathbb{P}_N - \mathbb{P}_{N-2}$ to prevent spurious pressure oscillations
  - $\mathbf{u}$: Gauss-Lobatto-Legendre (GLL) grid of order N
  - p: Gauss-Legendre (GL) grid of order $N-2$

- Time integrators
  - linear Stokes (viscous diffusive) term

    $\hookrightarrow$ implicit backward differential formula of order 2 (BDF2)
  - nonlinear convective term

    $\hookrightarrow$ explicit extrapolation of order 2 (EX2)

- Pressure treatments

  Generalized block LU decomposition

  $\hookrightarrow$ fractional-step method with pressure correction

Explicit filtering techniques: Modal filter

- Uses a modal hierarchical basis to ensure inter-elements $\mathcal{C}^0$-continuity of the filtered quantities

$$\phi_0 = \frac{1-\xi}{2}, \quad \phi_1 = \frac{1+\xi}{2}, \quad \phi_k = L_k(\xi) - L_{k-2}(\xi), \quad 2 \le k \le N$$

and the basis transfer reads $u(\xi_i) = \sum_{k=0}^{N} \widehat{u}_k \phi_k(\xi_i) \Leftrightarrow \mathbf{u} = \mathbf{\Phi}\widehat{\mathbf{u}}$

- Low-pass filtering performed in spectral modal space element-wise

$$\overline{\mathbf{u}} = G \star \mathbf{u} = \mathbf{\Phi} \mathbf{T} \mathbf{\Phi}^{-1} \mathbf{u} \quad \text{with} \quad T_k = \frac{1}{(1 + (k/k_c)^2)}$$

k_c cut-off value s.t $T_{k_c} = 1/2$

- Straightforward 3D extension by matrix tensor product

Explicit filtering techniques: Nodal filter and filter length

- Used to filter the highest frequencies to ensure stability of the simulation

$$\overline{u} = I_M^N \, I_N^M u \quad \text{with} \quad (I_N^M)_{ij} = h_{N,j}(\xi_{M,i})$$

where M is equal to $N-2$ or $N-3$

- Straightforward 3D extension by matrix tensor product

- Filter length based on $\Delta = s/p$ where s is the element size and p is the closest and lower polynomial degree to the cut-off k_c

- Straightforward 3D extension

$$\Delta(x,y,z) = (\Delta_1(x)\Delta_2(y)\Delta_3(z))^{1/3} = \left(\frac{s_1}{p_1}\frac{s_2}{p_2}\frac{s_3}{p_3}\right)^{1/3}$$

Physical and computational parameters 1/2

Domain size (x, y, z)	$(2h, 2h, 2h)$
Wall positions	$x,\ y,\ z = \pm h$
Reynolds number $\mathrm{Re} = U_0 2h/\nu$	$12\,000$
No. of spectral elements (E_x, E_y, E_z)	$(8, 8, 8)$
Polynomial orders (N_x, N_y, N_z)	$(8, 8, 8)$
Time step	$0.002\, h/U_0$
No. of iterations	$387\,000$
Length of simulation	$774 h/U_0$
Nodal filtering – DSM & DMM	$M = N - 2 = 6$
Modal filtering – DSM & DMM (1$^{\mathrm{st}}$ level)	$k_c = N - 2 = 6$
Modal filtering – DSM & DMM (2$^{\mathrm{nd}}$ level)	$k'_c = N - 3 = 5$

Table: Numerical and physical parameters of the simulations

Physical and computational parameters 2/2

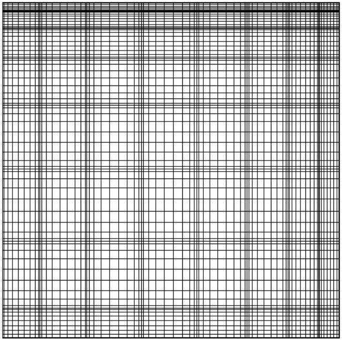

Figure: Spectral element grid in the mid-plane $z/h = 0$.

- Asymmetric distribution of elements to resolve high-gradients zones
- Equivalent to 65^3 grid points:

8 times less grid points than the reference DNS (129^3)

Physical and computational parameters 2/2

$$\mathcal{K}(t) = \int_{\mathcal{V}} \overline{\mathbf{u}}^2 \, \mathrm{d}\mathcal{V} \quad \text{and} \quad \kappa(t) = \int_{\mathcal{V}} \overline{\mathbf{u}}'^2 \, \mathrm{d}\mathcal{V}$$

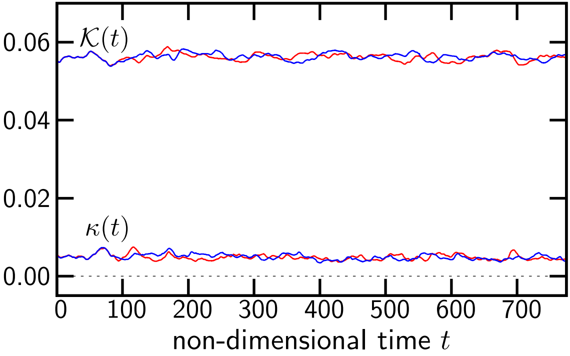

Figure: Time histories of $\mathcal{K}(t)$ and of $\kappa(t)$: LES-DSM (red lines) and LES-DMM (blue lines)

- Ensemble averaging taken equivalent to time averaging: steady turbulent state

Reynolds stress components in the mid-plane $z/h = 0$

- Experimental reference results from Prasad and Koseff at $\mathrm{Re} = 10\,000$:

  Prasad, A. K. & Koseff, J. R., Reynolds number and end-wall effects on a lid-driven cavity flow, *Phys. Fluids.*, **1** (2), 208–218, 1989.

- DNS reference results from Leriche and Gavrilakis at $\mathrm{Re} = 12\,000$:

  Leriche, E. & Gavrilakis, S., Direct numerical simulation of the flow in the lid-driven cubical cavity, *Phys. Fluids.*, **12**, 1363–1376, 1999.

Reynolds stress components in the mid-plane $z/h = 0$

- Experimental reference results from Prasad and Koseff at $\mathrm{Re} = 10\,000$: Crosses $+$
- DNS reference results from Leriche and Gavrilakis at $\mathrm{Re} = 12\,000$: Solid lines —
- LES-DSM: dashed lines $- - -$ and LES-DMM: dotted lines $\cdots$

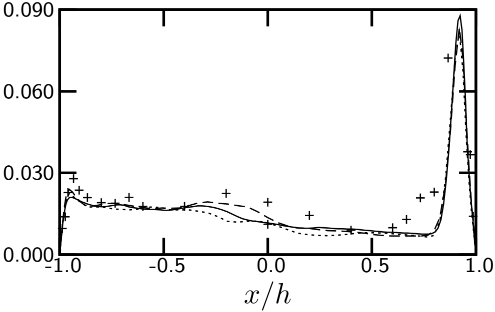

Figure: In the mid-plane $z/h = 0$: $\sqrt{\langle v^2 \rangle}$ on the horizontal centerline $y/h = 0$

Reynolds stress components in the mid-plane $z/h = 0$

- Experimental reference results from Prasad and Koseff at $\mathrm{Re} = 10\,000$: Crosses $+$
- DNS reference results from Leriche and Gavrilakis at $\mathrm{Re} = 12\,000$: Solid lines —
- LES-DSM: dashed lines $- - -$ and LES-DMM: dotted lines $\cdots$

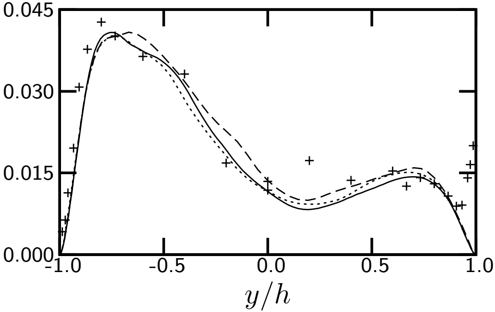

Figure: In the mid-plane $z/h = 0$: $\sqrt{\langle v^2 \rangle}$ on the vertical centerline $x/h = 0$

Reynolds stress components in the mid-plane $z/h = 0$

- Experimental reference results from Prasad and Koseff at $\mathrm{Re} = 10\,000$: Crosses $+$
- DNS reference results from Leriche and Gavrilakis at $\mathrm{Re} = 12\,000$: Solid lines —
- LES-DSM: dashed lines $- - -$ and LES-DMM: dotted lines $\cdots$

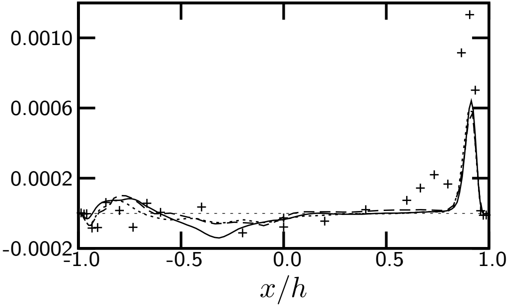

Figure: In the mid-plane $z/h = 0$: $\langle uv \rangle$ on the horizontal centerline $y/h = 0$

Reynolds stress components in the mid-plane $z/h = 0$

- Experimental reference results from Prasad and Koseff at $\mathrm{Re} = 10\,000$: Crosses $+$
- DNS reference results from Leriche and Gavrilakis at $\mathrm{Re} = 12\,000$: Solid lines —
- LES-DSM: dashed lines $---$ and LES-DMM: dotted lines $\cdots$

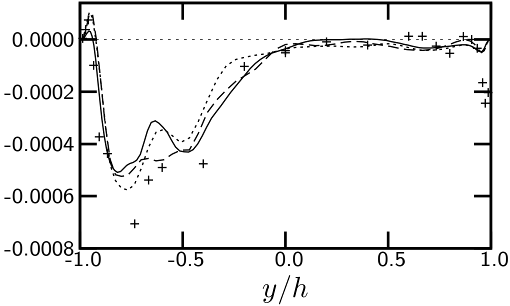

Figure: In the mid-plane $z/h = 0$: $\langle uv \rangle$ on the vertical centerline $x/h = 0$

First and second order moments in the mid-plane $z/h = 0$

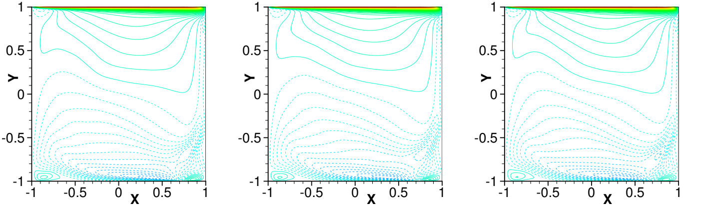

Figure: Contours of $\langle U \rangle$ in the mid-plane $z/h = 0$; DNS (left), LES-DSM (center) and LES-DMM (right)—100 contours levels taken between -0.4 and 1. Dashed contours lines correspond to negative levels

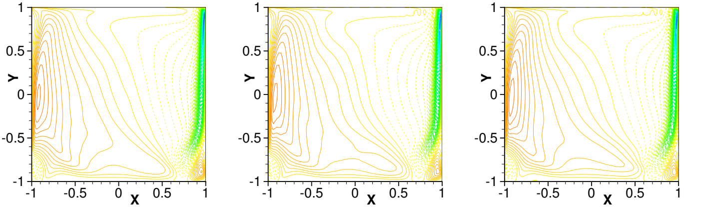

Figure: Contours of $\langle V \rangle$ in the mid-plane $z/h = 0$; DNS (left), LES-DSM (center) and LES-DMM (right)—100 contours levels taken between -0.7 and 0.2. Dashed contours lines correspond to negative levels

First and second order moments in the mid-plane $z/h = 0$

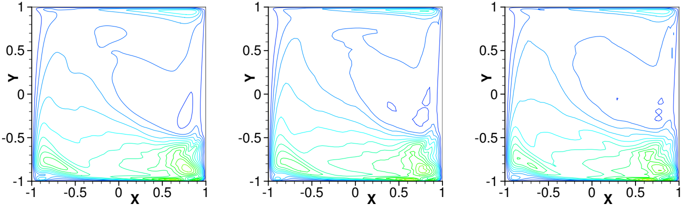

Figure: Contours of $\sqrt{\langle u^2 \rangle}$ of the velocity in the mid-plane $z/h = 0$; DNS (left), LES-DSM (center) and LES-DMM (right); 20 contours equally spaced between 0 and 0.1

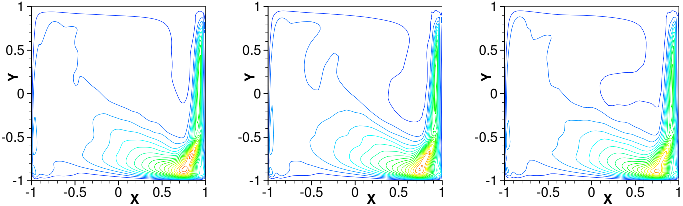

Figure: Contours of $\sqrt{\langle v^2 \rangle}$ of the velocity in the mid-plane $z/h = 0$; DNS (left), LES-DSM (center) and LES-DMM (right); 20 contours equally spaced between 0 and 0.15

Turbulence production near the downstream wall

- Largest turbulence production rates are to be found in the primary elliptical jets parallel to the downstream wall, near the impact points just above the bottom wall

$$P_{ij} = -\langle u_i u_k \rangle \frac{\partial \langle U_j \rangle}{\partial x_k} - \langle u_j u_k \rangle \frac{\partial \langle U_i \rangle}{\partial x_k}$$

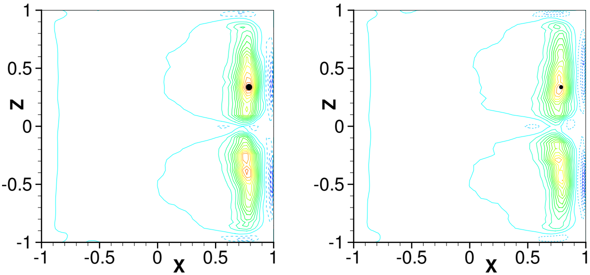

Figure: Term P_{22} in the plane $y/h = -0.9388$; DSM (left) and DMM (right); 20 contour levels $-0.025\,U_0^3/h$ and $0.070\,U_0^3/h$; dashed negative contour lines

Peaks of turbulence production

- Term $-v^2\partial\langle V\rangle/\partial y$ predominant in P_{22}:

$\hookrightarrow$ limited number of high-value peaks

$\hookrightarrow$ assumed to be engendered by specific coherent vortices

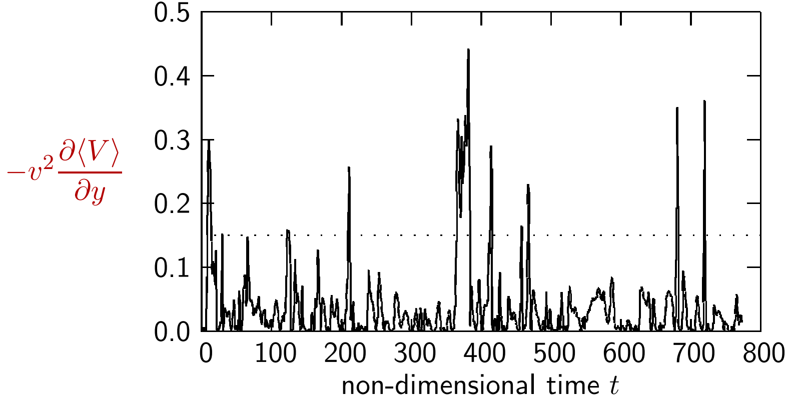

Figure: Time histories of the term $-v^2\partial\langle V\rangle/\partial y$ in U_0^3/h units for **LES-DSM**; the dotted lines represent the threshold value $0.15\,U_0^3/h$

Peaks of turbulence production

- Term $-v^2\partial\langle V\rangle/\partial y$ predominant in P_{22}:

↪ limited number of high-value peaks

↪ assumed to be engendered by specific coherent vortices

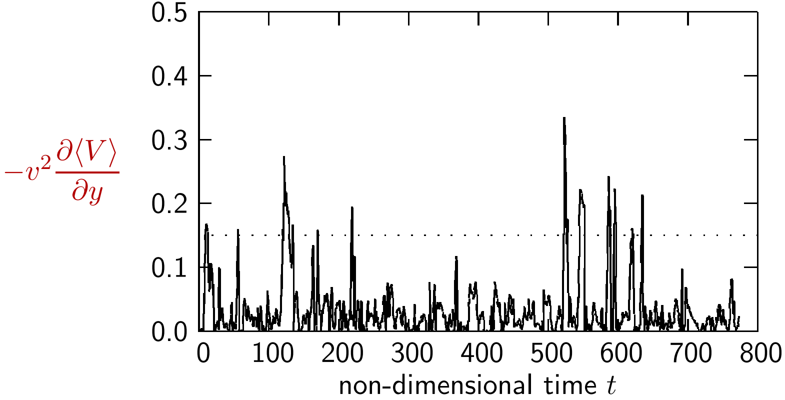

Figure: Time histories of the term $-v^2\partial\langle V\rangle/\partial y$ in U_0^3/h units for **LES-DMM**; the dotted lines represent the threshold value $0.15\,U_0^3/h$

Coherent structures responsible for the peaks of production

- Conditional averaging based on the threshold value $0.15\, U_0^3/h$ for $-v^2\partial\langle V\rangle/\partial y$

$\hookrightarrow$ Two counter-rotating vortices are clearly exhibited by both models above the bottom wall at $y/h = -1$

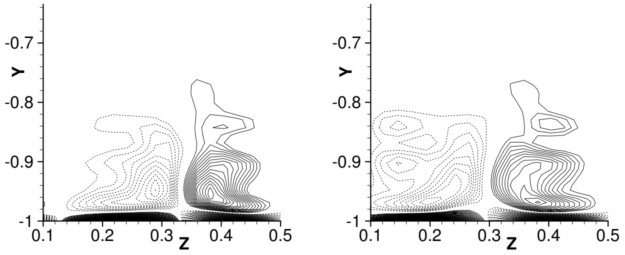

Figure: Contours of the conditionally averaged vorticity field $\langle\Omega_x\rangle_{\mathrm{ca}}$ in the plane $x/h = 0.7874$ for the LES-DSM (left) and the LES-DMM (right); dashed lines refer to negative contour levels

Small scales of the flow

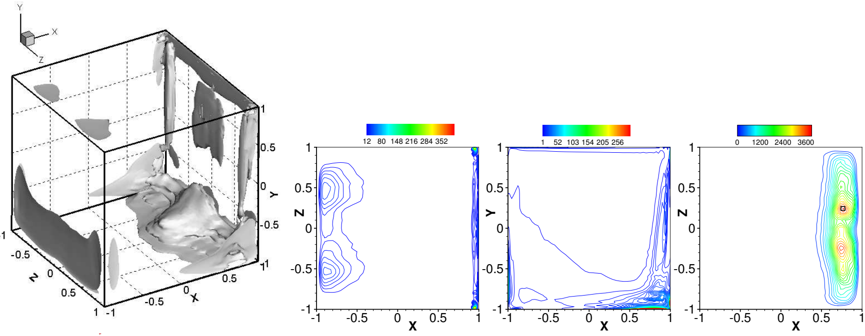

Figure: Visualization of the region of the cavity where the average turbulent energy dissipation rate $\langle\varepsilon\rangle$ is above 1% of its maximum value $3\,570\,\nu U_0^2/h^2$; LES-DMM; contour lines of $\langle\varepsilon\rangle$ in the following planes: lid-plane $y/h = 1$ (left), plane $z/h = 0.337$ (center), bottom-plane $y/h = -1$ (right); LES-DSM

Helical properties of the flow 1/3

- The helicity $\mathcal{H}$ is a measure of linkages and knots between the vorticity lines of the flow $\mathcal{H}(t) = \int_{\mathcal{V}} \mathbf{u} \cdot \boldsymbol{\omega} \, \mathrm{d}\mathcal{V}$

$\mathbf{u} \cdot \boldsymbol{\omega}$ is the helicity density. Both are pseudo-scalar quantities

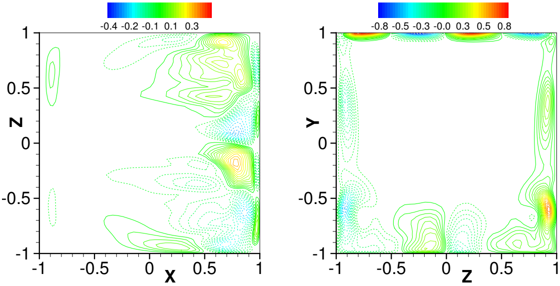

$\hookrightarrow$ allows to locate helical coherent structures

Figure: Contours of the average helicity density $\langle h \rangle$ in the bottom plane $y/h = -1$ (left) and in the plane $x/h = 0.7874$; LES-DSM

Helical properties of the flow 2/3

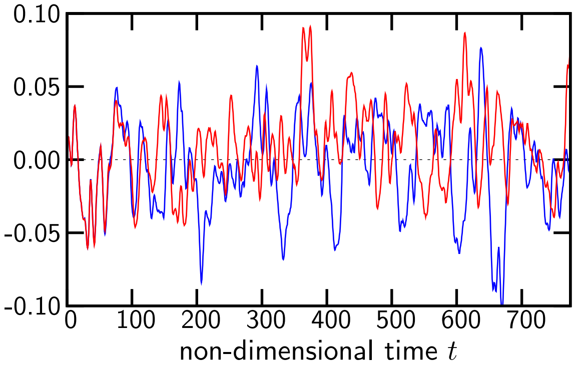

Figure: Time histories of $\mathcal{H}(t)$; LES-DSM (red lines) and LES-DMM (blue lines)

Helical properties of the flow 3/3

- Helicity, like energy, is cascaded from large scales down to the Kolmogorov scale, where it is dissipated
- Relative helicity spectrum α decreases at small scales just like homogeneous isotropic turbulence

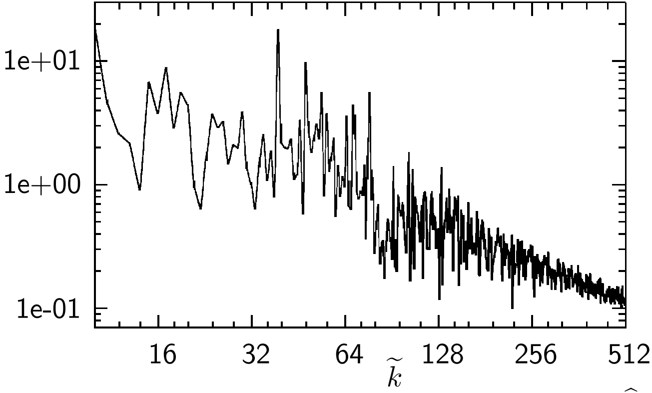

$$\alpha(\widehat{k}) = \frac{\widehat{\mathcal{H}}(\widehat{k})}{2\widehat{k}\,\widehat{\mathcal{K}}(\widehat{k})}$$

Figure: One-dimensional relative helicity spectrum $\alpha(\widehat{k})$; LES-DMM

Conclusions and future perspectives

- Comprehensive validation of DSM and DMM in the framework of SEM
- Both models are capable of capturing the very fine physics of this flow
- Ongoing approximate deconvolution model validation which are extremely encouraging
- With the same grid (65^3), LES of $\mathrm{Re} = 22\,000$ is in progress with DSM and DMM
- Ongoing **LES of turbulent free-surface flows** using these models

Additional data: MILES and Smagorinsky Model

- DNS reference results from Leriche and Gavrilakis at $\mathrm{Re} = 12\,000$: Solid lines —
- MILES: dashed lines $- - -$ and LES-SM: dotted lines $\cdots$

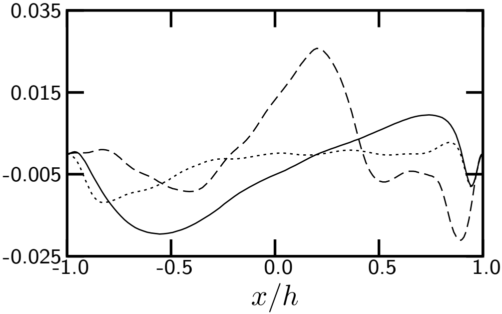

Figure: In the mid-plane $z/h = 0$: $\langle U \rangle$ on the horizontal centerline $y/h = 0$

Additional data: MILES and Smagorinsky Model

- DNS reference results from Leriche and Gavrilakis at $\mathrm{Re} = 12\,000$: Solid lines —
- MILES: dashed lines $---$ and LES-SM: dotted lines $\cdots$

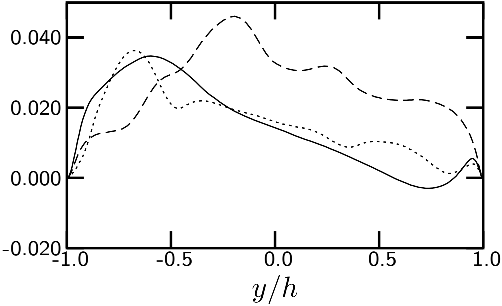

Figure: In the mid-plane $z/h = 0$: $\langle V \rangle$ on the vertical centerline $x/h = 0$

Additional data: MILES and Smagorinsky Model

- DNS reference results from Leriche and Gavrilakis at $\mathrm{Re} = 12\,000$: Solid lines —
- MILES: dashed lines $- - -$ and LES-SM: dotted lines $\cdots$

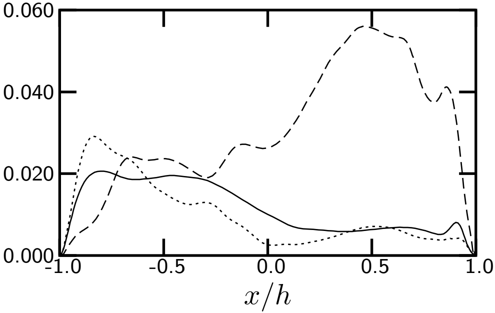

Figure: In the mid-plane $z/h = 0$: $\sqrt{\langle u^2 \rangle}$ on the horizontal centerline $y/h = 0$

Additional data: MILES and Smagorinsky Model

- DNS reference results from Leriche and Gavrilakis at $\mathrm{Re} = 12\,000$: Solid lines —
- MILES: dashed lines $- - -$ and LES-SM: dotted lines $\cdots$

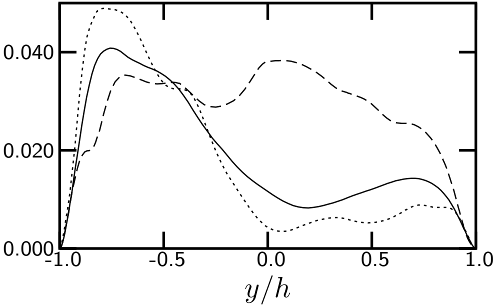

Figure: In the mid-plane $z/h = 0$: $\sqrt{\langle v^2 \rangle}$ on the vertical centerline $x/h = 0$

Dynamic Smagorinsky Model (DSM)

DSM overcomes the difficulty of constant C_{S}: dynamic constant $C_{\mathsf{d}} = C_{\mathsf{d}}(\mathbf{x}, t)$. Let us introduce a test-filter length scale $\widehat{\Delta}$ s.t. $\widehat{\Delta} = 2\overline{\Delta}$. Assuming that in the inertial range of the turbulence energy spectrum, the statistical self-similarity applies

$$\mathbf{T} = \widehat{\overline{\mathbf{u}\mathbf{u}}} - \widehat{\overline{\mathbf{u}}}\,\widehat{\overline{\mathbf{u}}}$$

The Germano identity gives $\mathbf{L} = \mathbf{T} - \widehat{\boldsymbol{\tau}} = \widehat{\overline{\mathbf{u}}\,\overline{\mathbf{u}}} - \widehat{\overline{\mathbf{u}}}\,\widehat{\overline{\mathbf{u}}}$ where the Leonard tensor $\mathbf{L}$ is directly computed from the resolved fields.
We apply the eddy-viscosity model to $\boldsymbol{\tau}$ and $\mathbf{T}$, same constant C_{d} and self-similarity hypothesis for C_{d}

$$\boldsymbol{\tau}^{\mathsf{d}} = -2C_{\mathsf{d}}\overline{\Delta}^2|\overline{\mathbf{S}}|\overline{\mathbf{S}} = C_{\mathsf{d}}\boldsymbol{\beta} \quad \text{and} \quad \mathbf{T}^{\mathsf{d}} = -2C_{\mathsf{d}}\widehat{\overline{\Delta}}^2|\widehat{\overline{\mathbf{S}}}|\widehat{\overline{\mathbf{S}}} = C_{\mathsf{d}}\boldsymbol{\alpha}$$

"d" denotes the deviatoric part of the tensor.

$$\mathbf{L}^{\mathsf{d}} = C_{\mathsf{d}}\boldsymbol{\alpha} - \widehat{C_{\mathsf{d}}\boldsymbol{\beta}}.$$

Assuming that C_{d} does not vary too much over an interval of dimension $\geq \widehat{\Delta}$, one sets $\widehat{C_{\mathsf{d}}\boldsymbol{\beta}} \approx C_{\mathsf{d}}\widehat{\boldsymbol{\beta}}$ and a least-square minimization leads to

$$C_{\mathsf{d}} = \frac{(\boldsymbol{\alpha} - \widehat{\boldsymbol{\beta}}) : \mathbf{L}^{\mathsf{d}}}{(\boldsymbol{\alpha} - \widehat{\boldsymbol{\beta}}) : (\boldsymbol{\alpha} - \widehat{\boldsymbol{\beta}})},$$

Dynamic Mixed Model (DMM)

DMM is a blend of the mixed model of Bardina and the former DSM. The mixed model is not an eddy-viscosity based model. Instead it belongs to the class of structural models and relies on the scale similarity principle. It produces almost no dissipation and for that reason needs to be used with the dynamic Smagorinsky model. By decomposing the velocity field as

$$\mathbf{u} = \overline{\mathbf{u}} + \mathbf{u}'$$

where $\mathbf{u}'$ represents the subgrid-scale velocity field and by inserting in Eq. (**??**), we can redefine the SGS stress as Germano [**?**] proposed

$$\boldsymbol{\tau} = \mathcal{L} + \mathcal{C} + \mathcal{R}, \tag{1}$$

where

$$\begin{aligned}
\mathcal{L} &= \overline{\overline{\mathbf{u}}\,\overline{\mathbf{u}}} - \overline{\overline{\mathbf{u}}}\;\overline{\overline{\mathbf{u}}}, \\
\mathcal{C} &= \overline{\overline{\mathbf{u}}\,\mathbf{u}' + \mathbf{u}'\,\overline{\mathbf{u}}} - (\overline{\overline{\mathbf{u}}}\;\overline{\mathbf{u}'} + \overline{\mathbf{u}'}\;\overline{\overline{\mathbf{u}}}), \\
\mathcal{R} &= \overline{\mathbf{u}'\,\mathbf{u}'} - \overline{\mathbf{u}'}\;\overline{\mathbf{u}'},
\end{aligned} \tag{2}$$

are designated as the modified Leonard stress, the SGS cross term, and the modified SGS Reynolds stress, respectively. The modified Leonard term can be calculated by resolved quantities and corresponds essentially to the mixed model. The two other terms are unresolved residual stresses and are treated

Space discretization

The spatial discretization uses Lagrange–Legendre polynomial interpolants. The semi-discrete filtered Navier–Stokes equations resulting from space discretization are

$$\begin{aligned} \mathbf{M}\frac{\mathrm{d}\underline{\overline{\mathbf{u}}}}{\mathrm{d}t} + \mathbf{C}\underline{\overline{\mathbf{u}}} + \nu\mathbf{K}\underline{\overline{\mathbf{u}}} - \mathbf{D}^T\underline{\overline{p}} + \mathbf{D}\underline{\boldsymbol{\tau}} &= 0, \\ -\mathbf{D}\underline{\overline{\mathbf{u}}} &= 0. \end{aligned}$$

The diagonal mass matrix $\mathbf{M}$ is composed of three blocks, namely the mass matrices M. The global vector $\underline{\overline{\mathbf{u}}}$ contains all the nodal velocity components while $\underline{\overline{p}}$ is made of all nodal pressures. The matrices $\mathbf{K}$, $\mathbf{D}^T$, $\mathbf{D}$ are the discrete Laplacian, gradient and divergence operators, respectively. The matrix operator $\mathbf{C}$ represents the action of the non-linear term written in convective form $\underline{\overline{\mathbf{u}}} \cdot \boldsymbol{\nabla}$, on the velocity field and depends on $\underline{\overline{\mathbf{u}}}$ itself.

Time discretization

The state-of-the-art time integrators in spectral methods handle the viscous linear term and the pressure implicitly by a backward differentiation formula of order 2 (BDF2) to avoid stability restrictions such that $\nu \Delta t \leq C/N^4$ while all non-linearities are computed explicitly, e.g. by a second order extrapolation method (EX2), under the CFL restriction $\overline{u}_{\text{max}} \Delta t \leq C/N^2$. Nonetheless, as the LES viscosity is not constant, we modify the standard time scheme in such a way that this space varying viscosity be handled explicitly

$$\nu_{\text{eff}} = \nu + \nu_{\text{sgs}} = \nu_{\text{cst}} + (\nu_{\text{eff}} - \nu_{\text{cst}}),$$

where ν_{cst} is the sum of the physical viscosity ν and the average of ν_{sgs} over the computational domain. The filtered semi-discrete Navier–Stokes equations become

$$\mathbf{M}\frac{\mathrm{d}\underline{\overline{\mathbf{u}}}}{\mathrm{d}t} + \nu_{\text{cst}}\mathbf{K}\underline{\overline{\mathbf{u}}} - \mathbf{D}^T\underline{\overline{p}} = -\mathbf{C}\underline{\overline{\mathbf{u}}} + 2\mathbf{D}(\nu_{\text{eff}} - \nu_{\text{cst}})\underline{\overline{\mathbf{S}}},$$

$$-\mathbf{D}\underline{\overline{\mathbf{u}}} = 0,$$

and the previous time splitting still applies. The viscous explicit term on the right-hand side does not harm stability as the magnitude of the term $2\mathbf{D}(\nu_{\text{eff}} - \nu_{\text{cst}})\underline{\overline{\mathbf{S}}}$ is less than that of $\mathbf{C}\underline{\overline{\mathbf{u}}}$.